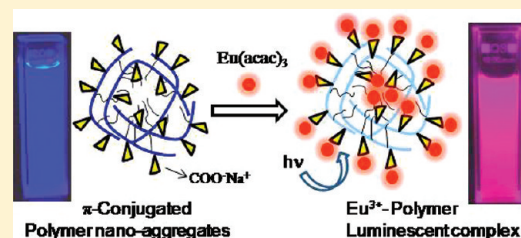


Amphiphilic π -Conjugated Poly(*m*-phenylene) Photosensitizer for the Eu^{3+} Ion: The Role of Macromolecular Chain Aggregation on the Color Tunability of Lanthanides

A. Balamurugan,[†] M. L. P. Reddy,[†] and M. Jayakannan^{*,†}[†]Chemical Sciences and Technology Division, National Institute for Interdisciplinary Science and Technology, Thiruvananthapuram-695019, Kerala, India[‡]Department of Chemistry, Indian Institute of Science Education and Research (IISER), Dr. Homi Bhabha Road, Pune 411008, India**S** Supporting Information

ABSTRACT: Here, we report new carboxylic functionalized poly-(phenylene)s and their oligomers as selective and efficient photosensitizers for Eu^{3+} ions. Palladium-catalyzed Suzuki polycondensation was developed for the synthesis of carboxylic functionalized π -conjugated materials. The chemical structures of the polymer skeleton were varied using two anchoring groups consisting of ethylhexyloxy and methoxy substitution in the chain backbone. The molecular weights of the polymer samples were obtained in the range of 4000–8000 containing 20 aromatic units in the chain. Photoexcitation of the oligomer- Eu^{3+} complexes resulted in magenta color emission as a result of the combination of partial blue self-emission from the chromophores along with the red color from the metal center. The ethylhexyl substituted polymer- Eu^{3+} complex showed complete excitation energy transfer from the macromolecular chains to the metal center and produced bright and sharp red emission. The polymer-containing methoxy unit was found to show largely self-emission rather than photoexcitation to the metal center. Singlet and triplet energy levels of the complexes and chromophores revealed that both oligomers and polymers have almost identical energy levels for photosensitizing Eu^{3+} ions. The polymers possessed typical amphiphilic structures via a rigid aromatic hydrophobic core and hydrophilic anionic periphery for self-organization in water. Both dynamic light scattering and atomic force microscope analysis confirmed the existence of the spherical shape nanometer size aggregates of the polymer chains in water. The branched ethylhexyl polymer showed the formation of loosely packed 500 nm aggregates whereas tightly packed 200 nm particles are produced by the methoxy substituted rigid polymer. These molecular aggregates behaved as templates for complexation as well as photosensitizing of the Eu^{3+} ions. The loosely packed nanoaggregates (ethylhexyl polymer) contain Eu^{3+} ions in the entire scaffold and showed efficient and complete energy transfer from the conjugated chain to metal ions. The tightly packed rigid-chains in methoxy polymer restricted the complete energy transfer to metal center. The molecular self-organization of the polymers played a crucial role on the efficient energy transfer from the polymer chain to metal center, more specifically Eu^{3+} ion-based red emission.



INTRODUCTION

Aromatic π -conjugated polymer-lanthanide hybrid materials are emerging as important candidates for the application in the field of light-emitting diodes.^{1,2} These hybrid materials possess unique features of both polymers and lanthanide complexes, for example, mechanical and thermal stability, flexibility, and a film-forming tendency of polymers along with unique optical properties of the lanthanides such as sharp emission, long lifetime, and high quantum yield.^{3–6} Additionally, the low absorption coefficients of the *f*-orbitals forbidden transitions in the lanthanides are also significantly improved by the strong absorbance characteristics of π -conjugated chains.⁷ Typically, two approaches are employed to make conjugated polymer–lanthanide hybrids: (a) blending of lanthanide complexes within π -conjugated polymers^{8–10} and (b) anchoring the lanthanide ions via chemical linkage at the polymer backbone.^{11–13} Although the physical

blending technique has been successfully explored for poly-(*p*-phenylene) and poly(fluorene) along with M^{3+} ions ($\text{M} = \text{Eu}$, Er , and Yb), the phase separation of metal ions from the organic polymeric matrix is being noticed as an inherent limitation.^{14,15} The chemical binding of M^{3+} ions with π -conjugated polymer chains were achieved via either functionalization of conjugated backbones or anchoring groups with appropriate units such as carboxylate,¹⁶ bipyridyl,¹⁷ or diketone.¹⁸ Similarly functionalized π -conjugated oligomers of fluorene, thiophene, and phenylene moieties were also explored for Eu^{3+} complexes.^{19–21} However, one of the most important unanswered fundamental questions is: what is the advantage of the π -conjugated polymeric ligands over

Received: May 11, 2011

Revised: July 31, 2011

Published: August 11, 2011

oligomers on the photosensitization of lanthanide ions? Though the polymers bring unique features such as processability and mechanical stability in the hybrid materials, it is very important and necessary to address the superiority of the photosensitizing ability of π -conjugated polymers over small molecular ligands. One of the obvious reasons routinely cited is the mis-match of the energy levels between the excited states (T_1) of the sensitizer (oligomer or polymer chain) to the excited state of the Eu^{3+} ions.²² For example, long conjugated polymer chains possessed a much lower HOMO–LUMO energy gap compared to that of its corresponding short oligomer. As a consequence for a particular chemical structure, only either a long chain polymer or oligomer was found as a suitable photoexcitation source. The lack of the availability of suitable chemical structures with identical energy levels in both oligomers and polymers hampered the study on the role of the macromolecular chain effect in the lanthanide ions. Therefore, a new molecular design with appropriate energy levels in both oligomer and polymer structures for lanthanide ions are high in demand. Recently, we have reported carboxylic functionalized poly(*m*-phenylenevinylene)s (*m*-PPV), their random copolymers, and structurally similar oligophenylenevinylene (OPV) as photosensitizers for Eu^{3+} and Tb^{3+} ions.²³ The co-complexation of the *m*-PPV polymer chain (blue) with both Eu^{3+} (red) and Tb^{3+} ions (green) resulted in the new generation of single polymer chain photosensitizers for white light emission.²³ However, the *m*-PPV polymer was found to be a good sensitizer for Eu^{3+} ions, whereas the OPV counterpart was not found suitable. This had limited our attempts to trace the effect of macromolecular chains over oligomers in lanthanide complexes. In our continual efforts to search for a new material design for the above purpose, here, we report new carboxylic functionalized poly(*m*-phenylene)s and oligophenylenes (both oligomer and polymer) as effective and selective photosensitizers for Eu^{3+} ions. This provides us with the opportunity to probe the importance of the π -conjugated macromolecular chain over the small molecular photosensitizer in the lanthanide ions.

The present work emphasizes the design and development of new carboxylic functionalized amphiphilic π -conjugated poly(*m*-phenylene)s and their oligomers. The chemical structures of the conjugated materials were designed based on phenylpropionic acid via tailor-made synthetic approaches. Palladium-mediated Suzuki polycondensation was adopted to make the polymer and oligomer sensitizers. The nature of the polymer was found as typical amphiphilic polyanion in water, and they exist as nanometer-sized self-organized aggregates. To probe the effect of the polymer structure on the molecular self-organization as well as their photosensitizing ability for lanthanide ions, the anchoring group in the chain backbone was varied using 2-ethylhexyloxy (branching units) or methoxy units. The structure of the oligomers, polymers, and their complexes were characterized by 1D-NMR, 2D-NMR, Fourier transform infrared (FT-IR), matrix-assisted laser desorption/ionization time-of-flight mass spectrometry (MALDI-TOF-TOF), thermogravimetric analysis (TGA), and so forth, and their molecular weights were determined by gel permeation chromatography (GPC). Absorption, emission, and time-resolved fluorescence decay techniques were employed to study the photosensitizing characteristics of the polymers and oligomers. Both oligomers and polymers showed selective photosensitization to Eu^{3+} ions among all of the lanthanides. The excitation energy transfer from the oligomer to Eu^{3+} ions resulted in magenta color emission from their complexes. The polymer showed complete energy transfer from

the macromolecular chain to Eu^{3+} ions, and pure red emission was obtained. Further the intrinsic quantum yield determined from time-resolved experiments revealed that the polymer complex was found highly luminescent compared to that of their oligomer complexes. Interestingly, the unique photosensitizing ability of the polymer chains was found highly dependent on the anchoring groups attached on the chain backbone and its influence on the molecular self-organization. Detailed studies by dynamic light scattering (DLS) and atomic force microscopy (AFM) revealed that the alkyl chain substitution on the polymer backbone influences their molecular self-organization. The size and nature of the nanoaggregates played a crucial role on the Eu^{3+} -polymer complex formation as well as their photosensitizing tendencies. In a nut shell, the present investigation provides direct evidence for the superior photosensitizing ability of the π -conjugated polymers over small molecules in the lanthanide ions, more specifically Eu^{3+} ions for red emission.

EXPERIMENTAL METHODS

Materials. 3-(4-Hydroxyphenyl)propionic acid, 2-ethylhexyl-bromide, 1,4-benzene bisboronic acid, tetrakis(triphenylphosphine) palladium(0), acetylacetone, $\text{Gd}(\text{NO}_3)_3 \cdot 6\text{H}_2\text{O}$, $\text{Tb}(\text{NO}_3)_3 \cdot 6\text{H}_2\text{O}$, and $\text{Eu}(\text{NO}_3)_3 \cdot 6\text{H}_2\text{O}$ were purchased from Aldrich Chemicals. K_2CO_3 , iodine, KI, methylamine, and all other reagents and solvents were purchased locally and purified following standard procedures.

General Procedures. ^1H NMR and ^{13}C NMR spectra of the monomers, oligomers, and the polymers were recorded using 400 MHz Joel NMR spectrophotometer in CDCl_3 containing a small amount of tetramethylsilane (TMS) as an internal standard. Infrared spectra of the oligomers, polymers, and their complexes were recorded using a Thermo-Scientific Nicolet 6700 FT-IR spectrometer with the solid state in KBr. The mass of all the oligomer Eu^{3+} complexes was confirmed by using the Applied Biosystems 4800 PLUS MALDI TOF/TOF analyzer. The molecular weight of the polymer and purity of the oligomers was determined by GPC using a Viscotek VE 1122 pump, Viscotek VE 3580 RI detector, and Viscotek VE 3210 UV/vis detector in tetrahydrofuran (THF) using polystyrene as a standard. The thermal stability of the polymeric complexes was determined using Perkin Elmer thermal analyzer STA 600 model at a heating rate of 10 °C/min in nitrogen atmosphere. The absorption and emission studies were done by a Perkin-Elmer Lambda 45 UV–visible spectrophotometer and SPEX Fluorolog HORIBA JOBIN VYON fluorescence spectrophotometer with a double-grating 0.22 m Spex1680 monochromator and a 450 W Xe lamp as the excitation source at room temperature. The excitation spectra are collected at 612 nm (Eu^{3+} ion emission wavelength), and the emission spectra are recorded by excitation at the excitation maxima. The size determination of the polymer solution is carried out by DLS, using a Nano ZS-90 apparatus utilizing 633 nm red laser (at 90° angle) from Malvern instruments. The reproducibility of the data was checked for at least three independent polymer solutions. The solution spectra of the sodium salt oligomers and polymers were recorded in water. The concentrations of the polymer and standard solution were adjusted in such a way to obtain the absorbance equal to 0.1 for the determination of quantum yield. The photoluminescence lifetime measurements were carried out at room temperature using a SPEX Fluorolog HORIBA JOBIN VYON 1934 D phosphorimeter. AFM images were recorded for drop caste

samples using JPK instruments attached with Nanowizard-II setup. AFM is also attached with a Zeiss inverted optical microscope.

Synthesis of 3-(4-Hydroxy-3,5-diiodophenyl)propanoic Acid (1). 3-(4-Hydroxyphenyl)propanoic acid (10.0 g, 60.2 mmol) was dissolved in 20% methylamine (100 mL) and stirred at room for about 15 min. KI (28.8 g, 173.6 mmol) and iodine (30.4 g, 120.3 mmol) in water (60 mL) were slowly added into the solution, and the stirring was continued for 5 h. The mixture was neutralized with 2 N concentrated HCl (100 mL), and the white precipitate was filtered and washed with water until the filtrate became neutral. The white solid was further purified by recrystallization from hot ethanol to obtain needle-like crystals as a product. Yield = 23.0 g (91%). $^1\text{H NMR}$ (400 MHz, CD_3OD) δ : 7.34 (s, 2H, Ar-H), 2.73 (t, 2H, Ar- CH_2CH_2), 2.51 (t, 2H, $\text{CH}_2\text{-CH}_2\text{COOCH}_3$). $^{13}\text{C NMR}$ (100 MHz, CD_3OD) δ : 178.92, 157.74, 143.12 (4C), 87.99, 39.16, and 32.52 ppm. FT-IR (KBr, cm^{-1}): 3460, 3060, 2920, 2850, 2550, 1710, 1540, 1450, 1400, 1340, 1300, 1230, 1130, 1030, 926, 879, 756, and 694. MALDI-TOF-TOF: MW = 417.97 and m/z = 440.9 ($\text{M}^+ + \text{K}^+$).

Synthesis of Methyl-3-(4-hydroxy-3,5-diiodophenyl)propanoate (2). Compound 1 (10.0 g, 120.0 mmol) was dissolved in dry methanol (50 mL) in 100 mL RB flask. Concentrated H_2SO_4 (6 mL) was slowly added into the methanol solution while stirring, and the mixture was refluxed for 6 h. It was concentrated and poured into water, and the precipitate was filtered and washed with water until the filtrate became neutral. The solid was redissolved in dichloromethane, washed with 5% NaHCO_3 , and dried over anhydrous Na_2SO_4 , and the solvent was evaporated to get a pale yellow solid as a product. It was further purified by crystallization from hot ethanol. Yield = 14.8 g (96%). $^1\text{H NMR}$ (400 MHz, CDCl_3) δ : 7.48 (s, 2H, Ar-H), 5.65 (s, 1H, Ar-OH), 3.64 (s, 2H, OCH_3), 2.78 (t, 2H, Ar- CH_2CH_2), 2.54 (t, 2H, $\text{CH}_2\text{-CH}_2\text{COOCH}_3$). $^{13}\text{C NMR}$ (100 MHz, CDCl_3) δ : 172.77, 152.04, 139.00 (4C), 136.56, 82.15, 51.74, 35.74, and 28.79. FT-IR (KBr, cm^{-1}): 3390, 2930, 2850, 1730, 1540, 1450, 1300, 1190, 1140, 972, 864, 787, and 694. MALDI-TOF-TOF: MW = 432.0 and m/z = 470.89 ($\text{M}^+ + \text{K}^+$).

Synthesis of Methyl-3-(4-(2-ethylhexyloxy)-3,5-diiodophenyl)propanoate (3). Compound 2 (5.0 g, 11.5 mmol) and anhydrous K_2CO_3 (34.5 g, 11.5 mmol) were dissolved in dry acetonitrile (60 mL) and then heated to 80 °C under nitrogen atmosphere for 1 h. After the addition of a catalytic amount of KI, 2-ethylhexyl bromide (17.7 g, (16.3 mL), 91.7 mmol) was slowly added into the reaction mixture for 15 min. The reaction was continued for 24 h at 80 °C under nitrogen atmosphere. The reaction mixture was poured into the water and extracted with ethyl acetate. The organic layer was washed with 5% NaOH, brine, and water and then dried over anhydrous Na_2SO_4 . The solvent was evaporated to get yellow liquid as product. It was purified by passing through silica gel column using hexane and 10% ethyl acetate as eluent. Yield = 16.9 g (70%). $^1\text{H NMR}$ (400 MHz, CDCl_3) δ : 7.59 (s, 2H, Ar-H), 3.80 (d, 2H, Ar- OCH_2), 3.68 (s, 3H, OCH_3), 2.82 (t, 2H, Ar- CH_2CH_2), 2.57 (t, 2H, $\text{-CH}_2\text{CH}_2\text{-COOCH}_3$), 1.93–0.91 (m, 15H, aliphatic H). $^{13}\text{C NMR}$ (100 MHz, CDCl_3) δ : 172.70, 156.51, 139.98, 139.68 (4C), 90.83, 76.10, 50.75, 40.26, 35.25, 30.08, 29.10, 29.01, 23.57, 23.08, 14.14, and 11.28. FT-IR (NaCl, liquid state, cm^{-1}): 2960, 2930, 2860, 1740, 1580, 1530, 1440, 1380, 1250, 1200, 1160, 1040, 989, 872, 831, 775, and 706. MALDI-TOF-TOF: MW = 544.21 and m/z = 582.90 ($\text{M}^+ + \text{K}^+$).

Synthesis of Methyl-3-(3,5-diiodo-4-methoxyphenyl)propanoate (4). Compound 2 (5.0 g, 11.6 mmol) and KOH (0.97 g, 17.4 mmol) were dissolved in dry methanol (10 mL) and stirred at ice-cold conditions. To the cold solution, dimethyl sulfate (2.2 g, 17.4 mmol) was slowly added. After the addition, the ice bath was removed, and the reaction mixture was heated to 70 °C for 3 h. The solid precipitate was poured into water and filtered, and the precipitate was washed with water until the filtrate became neutral. The product was further purified by crystallization from hot ethanol. Yield = 4.9 g (96%). $^1\text{H NMR}$ (400 MHz, CDCl_3) δ : 7.57 (s, 2H, Ar-H), 3.80 (s, 3H, Ar- OCH_3), 3.65 (s, 3H, OCH_3), 2.80 (t, 2H, Ar- CH_2CH_2), 2.56 (t, 2H, $\text{-CH}_2\text{CH}_2\text{-COOCH}_3$). $^{13}\text{C NMR}$ (100 MHz, CDCl_3) δ : 171.67, 157.27, 140.37, 139.60, 90.39, 60.67, 51.77, 32.22, and 20.02. FT-IR (KBr, cm^{-1}): 2926, 2890, 2371, 2330, 1729, 1574, 1531, 1447, 1407, 1358, 1300, 1167, 1055, 988, 858, 761, 703, 582, 577, and 443. MALDI-TOF-TOF: MW = 446.03 and m/z = 484.84 ($\text{M}^+ + \text{K}^+$).

Synthesis of 4,4,5,5-Tetramethyl-2-(4-(4,4,5,5-tetramethyl-1,3,2-dioxaborolan-2-yl)phenyl)-1,3,2-dioxaborolane (5). 1,4-Benzenediboronic acid (3.0 g, 18.1 mmol) and pinacol (4.3 g, 36.2 mmol) were dissolved in dry dichloromethane (60 mL) and then refluxed for 12 h under N_2 using a Dean–Stark apparatus. The organic layer was dried over anhydrous Na_2SO_4 , and the solvent was evaporated to get white solid product. The product was further purified by recrystallized from petroleum ether/chloroform mixture (v/v = 90:10). Yield = 4.7 g (80%). $^1\text{H NMR}$ (400 MHz, CDCl_3) δ : 7.78 (s, 4H, Ar-H), 1.33 (s, 24H, aliphatic H). $^{13}\text{C NMR}$ (100 MHz, CDCl_3) δ : 133.86, 83.83, 24.84. FT-IR (KBr, cm^{-1}): 2990, 2930, 1530, 1360, 1290, 1140, 1100, 1020, 957, 849, and 663. MALDI-TOF-TOF: MW = 330 and m/z = 331.35 (M^+).

Synthesis of Methyl-3-(3,5-diphenyl-4-methoxyphenyl)propanoate (OP-OM). Compound 4 (1.0 g, 2.3 mmol), 4-phenylboronic acid (0.7 g, 5.8 mmol), and $\text{Pd}(\text{PPh}_3)_4$ (0.04 g, 0.035 mmol) were dissolved in of dry THF (5 mL) under nitrogen purge. K_2CO_3 (1.3 g, 9.2 mmol) in water (1 mL, degassed with nitrogen) was added, and the mixture was stirred at 90 °C for 24 h. It was poured into water, extracted with ethyl acetate, and dried over anhydrous Na_2SO_4 . The liquid product was further purified by column chromatography using 5% ethyl acetate/petroleum ether as eluent. Yield = 0.68 g (88%). $^1\text{H NMR}$ (400 MHz, CDCl_3) δ : 7.59–7.57 (d, 4H, Ar-H), 7.42–7.40 (m, 4H, Ar-H), 7.34–7.30 (m, 2H, Ar-H), 7.17 (s, 2H, Ar-H), 7.59–7.17 (m, 12H, Ar-H), 3.68 (s, 3H, Ar- OCH_3), 3.13 (s, 3H, OCH_3), 2.99 (t, 2H, Ar- CH_2CH_2), 2.68 (t, 2H, $\text{-CH}_2\text{CH}_2\text{-COOCH}_3$). $^{13}\text{C NMR}$ (100 MHz, CDCl_3) δ : 173.30, 153.28, 138.58 (2C), 136.21, 135.64 (2C), 130.11 (2C), 129.24 (4C), 128.15 (4C), 127.11 (2C), 60.47, 51.69, 35.70, and 30.35. FT-IR (NaCl, liquid state, cm^{-1}): 3040, 2930, 2850, 2380, 1740, 1600, 1430, 1370, 1230, 1170, 1020, 879, 756, and 694. MALDI-TOF-TOF: MW = 346.46 and m/z = 385 ($\text{M} + \text{K}^+$).

Synthesis of Methyl-3-(3,5-diphenyl-4-(2-ethylhexyloxy)phenyl)propanoate (OP-OE). Compound 3 (1.0 g, 1.8 mmol) was reacted with 4-phenylboronic acid (0.6 g, 4.6 mmol) and K_2CO_3 (1.0 g, 7.4 mmol) using $\text{Pd}(\text{PPh}_3)_4$ (0.04 g, 0.03 mmol) as a catalyst THF + water mixture (5 + 1 mL) following the procedure described for OP-OM. The product was purified by column chromatography using 5% ethyl acetate/petroleum ether as eluent. Yield = 0.61 g (75%). $^1\text{H NMR}$ (400 MHz, CDCl_3) δ : 7.56–7.55 (d, 4H, Ar-H), 7.38–7.36 (m, 4H, Ar-H),

7.32–7.30 (m, 2H, Ar–H), 7.14 (s, 2H, Ar–H), 3.66 (s, 3H, Ar–OCH₃), 3.01 (d, 2H, OCH₂), 2.97 (t, 2H, Ar–CH₂CH₂), 2.66 (t, 2H, –CH₂CH₂–COOCH₃), 1.23–0.37 (m, 15H, aliphatic H). ¹³C NMR (100 MHz, CDCl₃) δ: 173.30, 153.28, 138.58 (2C), 136.21, 135.64 (2C), 130.11 (2C), 129.24 (4C), 128.15 (4C), 127.11 (2C), 60.47, 51.69, 35.70, and 30.35. FT-IR (NaCl, liquid state, cm⁻¹): 3040, 2930, 2870, 2380, 1740, 1600, 1430, 1370, 1220, 1170, 1020, 879, 756, and 694. MALDI-TOF TOF: MW = 444.62 and *m/z* = 483.22 (M + K⁺).

Synthesis of Poly[methyl-3-(4-(2-ethylhexyloxy)phenyl)-alt-(1,4-phenylene)propanoate] (PP-OE). Compound 3 (0.54 g, 1.0 mmol), compound 5 (0.33 g, 1.0 mmol), and Pd(PPh₃)₄ (0.04 g, 0.03 mmol) were dissolved in dry THF (4 mL). K₂CO₃ (0.55 g, 4.0 mmol) in water (1 mL, degassed with nitrogen) was added, and the polymerization was proceeded by stirring at 90 °C for 24 h. It was poured into methanol, filtered, and purified by dissolved in THF and reprecipitated into methanol. The polymer was dried in vacuum oven at 45 °C. Yield = 0.23 g (63%). ¹H NMR (400 MHz, CDCl₃) δ: 7.76–7.67 (m, 4H, Ar–H), 7.24 (broad s, 2H, Ar–H), 3.69 (s, 3H, Ar–OCH₃), 3.15 (d, 2H, OCH₂), 3.02 (t, 2H, Ar–CH₂CH₂), 2.72 (t, 2H, –CH₂CH₂–COOCH₃), 1.3–0.40 (m, 15H, aliphatic H). ¹³C NMR (100 MHz, CDCl₃) δ: 173.38, 153.01, 138.58, 135.97, 135.95, 130.03 (2C), 129.20 (2C), 127.44, 127.39, 126.58, 75.21, 51.70, 40.12, 35.78, 30.43, 30.21, 29.68, 28.94, 23.43, 23.38, 23.32, 22.98, 22.83, 14.08 (2C), 11.05, 10.88, and 10.83. FT-IR (KBr, cm⁻¹): 3390, 2960, 2920, 2870, 1740, 1580, 1450, 1380, 1220, 1180, 1010, 918, 837, and 741. GPC: *M_n* = 4000, *M_w* = 7900, and *M_w*/*M_n* = 1.9.

Synthesis of Poly[methyl 3-(4-methoxyphenyl)-alt-(1,4-phenylene)propanoate] (PP-OM). Compound 4 (0.50 g, 1.1 mmol), compound 5 (0.37 g, 1.1 mmol), and Pd(PPh₃)₄ (0.04 g, 0.03 mmol) were dissolved in dry THF (4 mL). K₂CO₃ (0.62 g, 4.50 mmol) in water (1 mL, degassed with nitrogen) was added, and the rest of the polymerization procedure is the same as described for PP-OE. Yield = 0.12 g (40%). ¹H NMR (400 MHz, CDCl₃) δ: 7.66–7.60 (m, 4H, Ar–H), 7.24 (broad s, 2H, Ar–H), 3.67 (s, 3H, Ar–OCH₃), 3.23 (s, 3H, OCH₃), 3.01 (t, 2H, Ar–CH₂CH₂), 2.71 (t, 2H, –CH₂CH₂–COOCH₃). ¹³C NMR (100 MHz, CDCl₃) δ: 173.33, 153.52, 137.44, 136.32, 135.37, 130.16, 129.25, 129.07, 60.58, 51.71, 35.75, and 30.40. FT-IR (KBr, cm⁻¹): 3020, 2930, 2870, 1740, 1600, 1450, 1370, 1230, 1170, 1020, 849, 756, and 694. GPC: *M_n* = 2300, *M_w* = 4100, and *M_w*/*M_n* = 1.4.

Synthesis of Eu³⁺ Complexes. The polymers or oligomers were dissolved hydrolyzed into their corresponding sodium salts in THF/MeOH. NaOH (2 mol equiv) in water was added to the solution, and the mixture was refluxed for 12 h at 70 °C. Acetylacetone (0.07 g, 0.67 mmol) was dissolved in ethanol (5 mL), and NaOH (0.03 g, 0.67 mmol) in water was added into the in situ prepared sodium salt polymer or oligomer (0.23 mmol). The whole mixture was stirred well for about 30 min, and Eu(NO₃)₃·6H₂O (0.1 g, 0.23 mmol) in ethanol (1 mL) was slowly added into the mixture. The complex was precipitated in water, filtered and washed with water and hot ethanol, and dried in a vacuum oven.

Eu(acac)₃(OP-OM). EtOH: Yield = 0.14 g, (61%). FT-IR (KBr, cm⁻¹): 3430, 2930, 2870, 1570, 1430, 1220, 1020, 870, 756, and 694. MALDI-TOF TOF: MW = 850.53 and *m/z* = 851.51.

Eu(acac)₃(OP-OE). EtOH: Yield = 0.15 g, (66%). FT-IR (KBr, cm⁻¹): 3430, 3040, 2930, 2870, 2350, 1570, 1430, 1220,

1020, 895, 756, and 694. MALDI-TOF TOF: MW = 965.31 and *m/z* = 965.53.

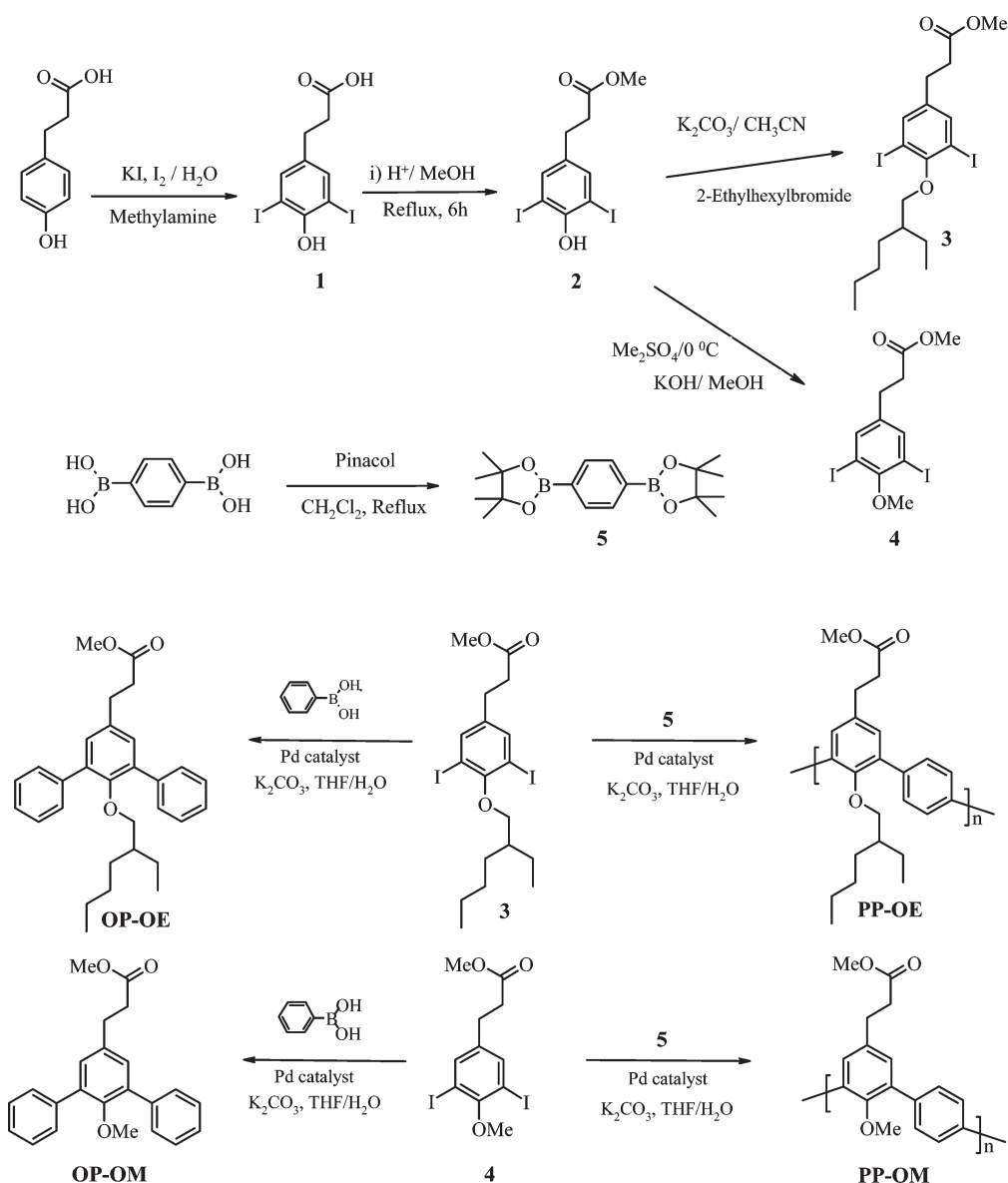
Eu(acac)₃(PP-OM). Yield = 0.08 g, (62%). FT-IR (KBr, cm⁻¹): 3400, 2950, 2930, 2870, 1540, 1450, 1390, 1250, 1000, 870, 781, and 698.

Eu(acac)₃(PP-OE). Yield = 0.10 g, (45%). FT-IR (KBr, cm⁻¹): 3360, 2930, 1600, 1520, 1460, 1400, 1260, 1190, 1020, 916, 766, and 658.

RESULTS AND DISCUSSION

Synthesis and Structural Characterization. Carboxylic acid functionalized monomers, oligomers, and polymers were synthesized as shown in Scheme 1. 3-(4-Hydroxyphenyl)propionic acid was used as starting material and iodinated with KI/I₂ in the presence of 20% methylamine in water to get the compound 3-(4-hydroxy-3,5-diiodophenyl)propanoic acid (1). The carboxylic acid of compound 1 was protected as methyl ester by acid catalyzed esterification reaction in the presence of concentrated H₂SO₄ in methanol to yield methyl 3-(4-hydroxy-3,5-diiodophenyl)propionate (2). 2 was further reacted with 2-ethylhexyl bromide or dimethyl sulfate to yield 3-[3,5-diiodo-4-(2-ethylhexyl)] propionate (3) and 3-(3,5-diiodo-4-methoxyphenyl)propionate (4), respectively. 1,4-Benzenebisboronic acid was converted into pinacol ester (5). π -Conjugated poly(*m*-phenylene)s and oligophenylenes were synthesized by palladium mediated Suzuki coupling polymerization method as shown in Scheme 1. Equimolar amounts of monomer 3 were polymerized with pinacol ester of benzenebisboronic acid (5) in the presence of K₂CO₃ in THF/H₂O using Pd(PPh₃)₄ as a catalyst to obtain the polymer poly[methyl-3-(4-(2-ethylhexyloxy)-phenyl)-alt-(1,4-phenylene)propanoate] (PP-OE). Similarly 4 was reacted with 5 to obtain the polymer poly[methyl 3-(4-methoxyphenyl)-alt-(1,4-phenylene)propanoate] (PP-OM). Structurally identical two oligophenylene derivatives methyl-3-(3,5-diphenyl-4-methoxyphenyl)propanoate (OP-OM) and 3-(3,5-diphenyl-4-(2-ethylhexyloxy)phenyl)propanoate (OP-OE) were obtained by reacting 3 and 4 with two equivalents of phenylboronic acid. The polymers and oligomers are referred as PP-OX and OP-OX, respectively, where PP = polyphenylene, OP = oligophenylene, and X = E and M (E = ethylhexyl and M = methyl unit). The structures of monomers, oligomers, and polymers were confirmed by ¹H NMR, ¹³C NMR, and HSQC-DEPT 135 NMR spectroscopic analysis. ¹H NMR and ¹³C NMR spectra of oligophenylene OP-OE and its corresponding polymer PP-OE are shown in Figure 1. In Figure 1a, the doublet at 7.56 and two multiplets at 7.38 and 7.30 ppm were assigned to terminal phenyl rings. The aromatic proton in the central ring appeared as singlet at 7.13 ppm. To further confirm the formation of the expected structure, the oligomer OP-OE was subjected to ¹H–¹³C coupled 2D NMR (HSQC-DEPT 135 technique) (see Figure S8 in the Supporting Information). The ¹³C NMR spectra on the right-hand side of the 2D plot possessed features of the DEPT 135 for the carbons atoms. For example, the carbon attached with odd number of protons appeared in the upward direction, whereas these attached with an even number of protons appeared in a downward direction. On the basis of the 2D NMR analysis, carbon atoms in Figure 1c were assigned in the OP-OE oligomer. Carbon atoms in Ar–CH₂CH₂COOCH₃ appeared at 30.5, 35.8, and 51.7 ppm, respectively. Other carbon atoms with respect to ethylhexyl units appeared well at below 30 ppm. The peaks for aryl carbon atoms appeared above 120 ppm.

Scheme 1. Synthesis of Monomers, Oligomers, and Polymers



On the basis of the 2D experiment (see expanded plots in the Supporting Information, Figure S8), the carbon atoms for 9, 10, 11, and 6 were assigned at 129.6, 128.0, 127.0, and 130.1 ppm, respectively. The carbonyl carbon atom in the C=O unit appeared at 172.2 ppm (see Figure 1c). The remaining four peaks at 152.8, 138.8, 136.3, and 135.9 were assigned to other four aryl carbon atoms 5, 7, 8, and 12, respectively. ¹H and ¹³C NMR spectra of polymer PP-OE are shown along with the oligomer in the figure 1. In the polymer structure, the aryl protons in the 1,4-phenyl ring are not identical because of the unsymmetrical substitution in the neighboring *m*-phenylene ring. As a consequence, the aromatic protons 10 and 10' in Figure 1b appeared as close doublets at 7.76–7.67 ppm. The aromatic proton in the 1,3-phenylene ring appeared as board peak along with solvent at 7.20 ppm. ¹³C NMR spectrum of the polymer possessed required number of peaks as similar to their structurally identical oligomer OP-OE. Similarly, the structure of the

methoxy substituted polymer PP-OM and its oligomer OP-OM were also confirmed by the NMR spectroscopy, and the details are provided in the Supporting Information (see Figure S6). The detailed ¹H, ¹³C, and 2D NMR techniques confirmed the formation of the expected structure both in the polymers and structurally identical oligomers.

Molecular Weight of the Polymers. The molecular weights of the polymers were determined by GPC in THF solvent, and their *M_n*, *M_w*, and polydispersity are given along with their GPC chromatograms in Figure 2. The GPC chromatograms appeared as a single peak indicating the formation of uniformly dispersed polymers for Pd(PPh₃)₄ mediated Suzuki polycondensation. The molecular weights of the polymers were found as moderate with the average number of repeating units of *n* = 9–12 in the conjugated backbone. To study the role of the catalyst on the molecular weight of the chains, the Suzuki polycondensation was also carried out using Pd(OAc)₂ as a catalyst. However, the

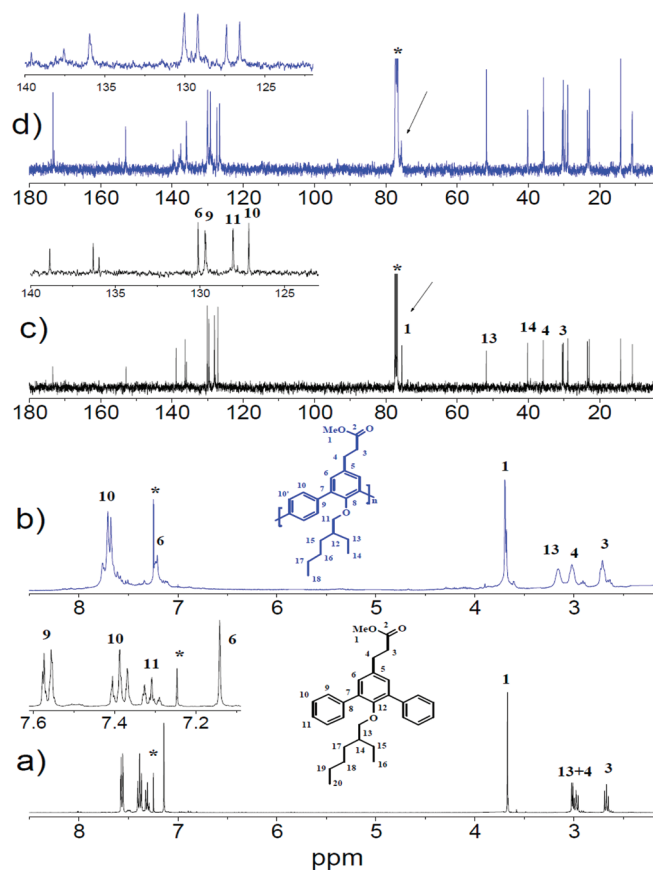


Figure 1. ^1H NMR (expanded) and ^{13}C NMR of OP-OE (a and c) and PP-OE (b and d) in CDCl_3 .

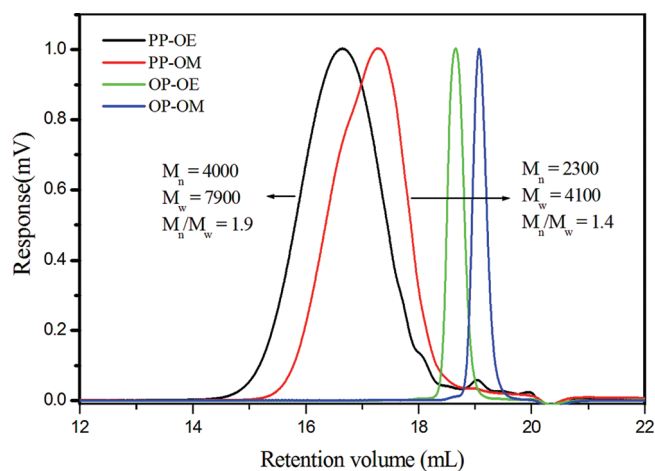


Figure 2. GPC chromatogram of the polymers and oligomers in THF at 30°C .

molecular weight was found at much lower values for the $\text{Pd}(\text{OAc})_2$ assisted process compared to that of the $\text{Pd}(\text{PPh}_3)_4$ ($M_n = 1600$, $M_w = 2100$, see GPC data for Supporting Information, Figure S9). The incorporation of a 1,3-unit in the conjugated polymeric chains may inherently limit the formation of high molecular weight polymers due to steric hindrance. A similar trend was earlier observed by us as well as others in the polycondensation of meta-linkage π -conjugated polymers.^{23,24}

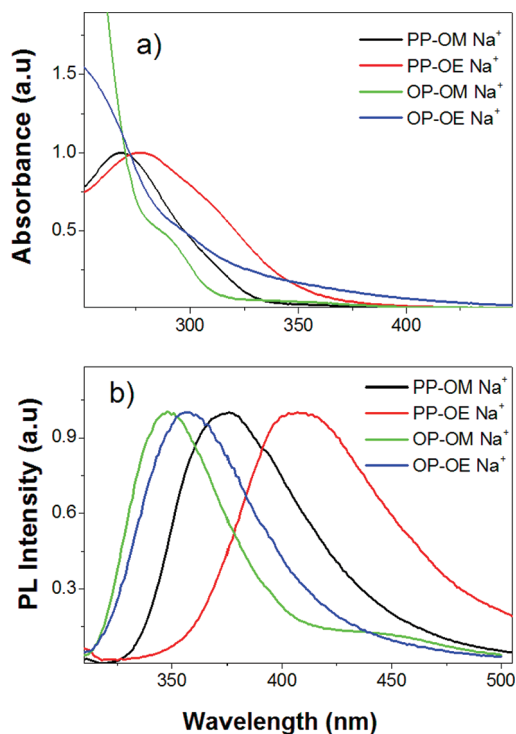


Figure 3. Absorption (a) and emission (b) spectra of sodium salt of polymers and oligomers at $1 \times 10^{-6} \text{ M}^{-1}$ in water.

The molecular weight of the ethylhexyloxy polymer (PP-OE) was found to be much higher ($M_w = 7900$) compared to that of the methoxy polymer (PP-OM, $M_w = 4100$). The reason for the formation of the high molecular weight in the PP-OE is attributed to the high solubility induced by the branched ethylhexyl units compared to that of the $-\text{OMe}$ units in the backbone. The photophysical properties of the π -conjugated polymers are known to attain the maxima at oligomers with 6–8 aryl units.²⁴ In the present system, the average chain length of $n = 9$ –12 carries almost 18–22 aryl units in the polyphenylene chains which is sufficient enough for the studying their photophysical characteristics. The GPC chromatograms of the oligomers were also shown along with the polymers in Figure 2. The oligomers showed a single peak indicating the high purity of the samples, and their mass was also confirmed by MALDI-TOF analysis (see Supporting Information, Figure S7).

Photophysical Properties of the Conjugated Materials. π -Conjugated polymers are typically water-insoluble; however, the carboxylic functional group attached in the polymer increases their water solubility. Since the complexation of lanthanide ions with the polymer chromophores was carried out in aqueous conditions, it is more appropriate to study their photophysical characteristics in water rather than other solvents. Therefore, the ester groups in oligomers and polymers were hydrolyzed into their corresponding carboxylic acid sodium salts. The solution absorbance and emission spectra of the sodium salts of polymer and oligomers in water are shown in Figure 3. Both OP-OE and OP-OM oligomers showed broad absorbance at 270–285 nm. The methoxy substituted polymer PP-OM showed almost identical absorbance with the oligomers; however, its ethylhexyl counterpart PP-OE showed 20 nm red shifts. Emission maxima of the polymers and oligomers were found to follow the order OP-OM < OP-OE < PP-OM < PP-OE. The polymers showed

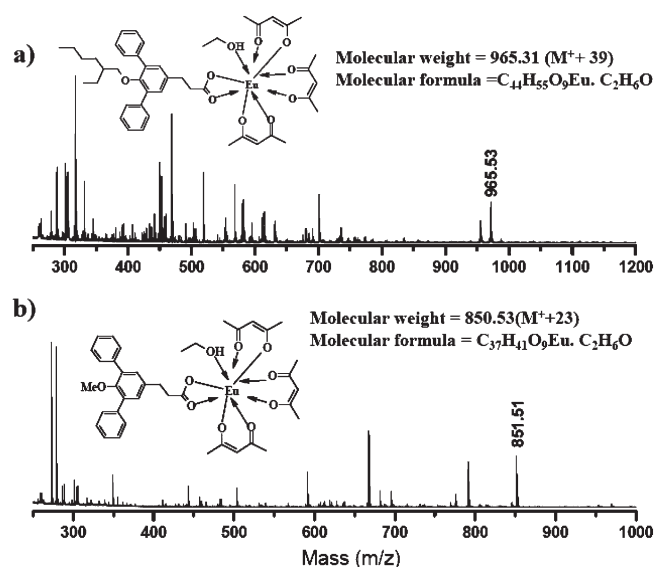


Figure 4. MALDI-TOF spectra of Eu^{3+} complexes of oligomers.

more red-shifted compared to that of their oligomers, and among the polymers the ethylhexyl polymer PP-OE showed a larger red shift. The large difference in the emission properties of the samples suggest that, despite the polymer and oligomers possessing identical 1,3-phenylene linkage, their emission characteristics are different with respect to their structural features in the chain length or anchoring groups. For instance, the branched anchoring ethylhexyl polymer PP-OE has a strong tendency for the aggregation which is clearly evident from the appearance of a shoulder in the absorbance spectrum at 310 nm as well as a 60 nm red-shift in the emission spectrum. On the other hand the photophysical characteristics of methoxy substituted rigid polymer PP-OM are almost similar to that of the oligomer OP-OM (also OP-OE). The absorbance and emission spectra of the polymers and oligomers in their carboxylic acid form in the THF were found almost identical (see Figure S17, Supporting Information) to that of their trend in Figure 3. This suggests that newly synthesized polymers were very stable in both acid form (in organic good solvent, like THF) as well as sodium salt form in water.

Synthesis and Characterization of Eu^{3+} Complexes. Carboxylic acid functionalized polyphenylene and its oligomers were employed as chromophores for Eu^{3+} complexes using acetylacetonate as coligands. Three mole equivalents of acetyl acetone (as coligand) and one mole equivalent of $\text{Eu}(\text{NO}_3)_3 \cdot 6\text{H}_2\text{O}$ in ethanol were complexed with sodium salts of polymers and oligomers. The resultant complexes were precipitated and purified by washing with hot ethanol and water. Oligomeric Eu^{3+} complexes were purified by recrystallization from dichloromethane. The formation of Eu^{3+} complexes was confirmed by FT-IR spectroscopic techniques (see Supporting Information, Figure S10). The peak corresponding to the $\text{C}=\text{O}$ bond stretching frequency at 1740 cm^{-1} in the polymer (also oligomer) completely vanished, and new peaks at 1600 and 1520 cm^{-1} with respect to symmetric and antisymmetric vibrations of Eu^{3+} metal coordinated $\text{C}=\text{O}$ carboxylate group appeared.²⁵ To confirm the structure and molecular weight of oligomeric complexes, the solid samples were subjected to high resolution MALDI-TOF-TOF analysis using 2,4-dihydroxybenzoic acid as a matrix (see Figure 4). The mass spectrum of

$\text{Eu}(\text{acac})_3(\text{OP-OE})(\text{EtOH})$ showed peaks at 949.56 and 965.53 amu with respect to its sodium and potassium ion peaks. Similarly, the methoxy substituted oligomer complex, $\text{Eu}(\text{acac})_3(\text{OP-OM})(\text{EtOH})$ showed a molecular ion peak at 851.53 with respect to its sodium ion peak. Both complexes exhibit the presence of ethanol molecule in the coordination sphere which satisfies the 9-coordination of Eu^{3+} ions in the complex. Our attempt to grow single crystals for the complex was not successful so far. Nevertheless, the mass spectra analyses of the complex proved the formation of Eu^{3+} complex with the newly synthesized oligophenylenes. The thermal stability of the polymer, oligomer, and their complexes were characterized by thermogravimetric analysis (see Supporting Information, Figure S11). The polymers, oligomers, and their Eu^{3+} complexes were stable up to $290\text{--}350\text{ }^\circ\text{C}$.

Excitation and emission spectra of Eu^{3+} complexes were recorded at room temperature (298 K) in the powder state, and the spectra for the oligomer complexes are shown in Figure 5. Excitation spectra showed broad maxima corresponding to aromatic π -conjugated core and weak sharp metal absorption peaks at 380, 393, and 417 nm as a resultant of transition between ground state (${}^7\text{F}_5$) to higher energy states. The emission spectra were recorded by exciting the samples at excitation maxima. Upon excitation, there are two types of emission are possible in complexes: (i) broad self-emission of conjugated chromophore in the blue region and (ii) excitation energy transfer from conjugated chromophore to metal ions and subsequent Eu^{3+} metal centered sharp emission in the range of $570\text{--}720\text{ nm}$.²⁶ The emission spectra of the $\text{Eu}(\text{acac})_3(\text{OP-OE})$ complex showed very strong ${}^5\text{D}_0$ state emissions centered at 612 nm with very small self-emission of the OP-OE in the range of $350\text{--}450\text{ nm}$. The sharp metal emission peaks at 579, 590, 615, 649, and 699 nm were attributed to ${}^5\text{D}_0 \rightarrow {}^7\text{F}_0$, ${}^5\text{D}_0 \rightarrow {}^7\text{F}_1$, ${}^5\text{D}_0 \rightarrow {}^7\text{F}_2$, ${}^5\text{D}_0 \rightarrow {}^7\text{F}_3$, and ${}^5\text{D}_0 \rightarrow {}^7\text{F}_4$ transitions, respectively.²⁶ The emission spectra of methoxy oligomer complex $\text{Eu}(\text{acac})_3(\text{OP-OM})$ were found almost similar to that of its ethylhexyl counterpart. The photographs of the emission for the complex (solid powder and dispersed in DMSO solution) were taken by excitation with a hand-held UV lamp (excitation = 365 nm light). The photographs for the oligomer complexes are shown along with their emission spectra in Figure 5. The weak partial blue self-emission of the oligomer chromophores resulted in magenta color emission from the Eu^{3+} -oligomer complex. The emission spectra of the polymer complexes are shown in Figure 6. The ethylhexyl substituted polymer complex $\text{Eu}(\text{acac})_3(\text{PP-OE})$ showed complete energy transfer from the macromolecular chain chromophore to Eu^{3+} metal centered, and sharp and intense red emission at 613 nm was observed. On the other hand, the emission spectrum of the methoxy polymer complex $\text{Eu}(\text{acac})_3(\text{PP-OM})$ was found to show very strong self-emission in the range of $350\text{--}450\text{ nm}$ along with relatively weak emission from the metal center at 612 nm. The comparisons of the emission spectra of polymer complexes suggest that ethylhexyl polymer (PP-OE) is a very good sensitizer compared to its methoxy counterpart. To check the selectivity of the chromophores among lanthanide metals, the samples were checked for sensitizing Tb^{3+} , Sm^{3+} , and Dy^{3+} ions. The samples showed selectivity only for Eu^{3+} ions, and no energy transfer was observed in other lanthanide complexes (see Figure S14, Supporting Information). The CIE chromaticity diagram for the Eu^{3+} complexes generated by feeding their emission spectra and the color coordinates were determined. The ethylhexyl polymer PP-OE produced $x = 0.61$ and $y = 0.31$ which are almost close to the

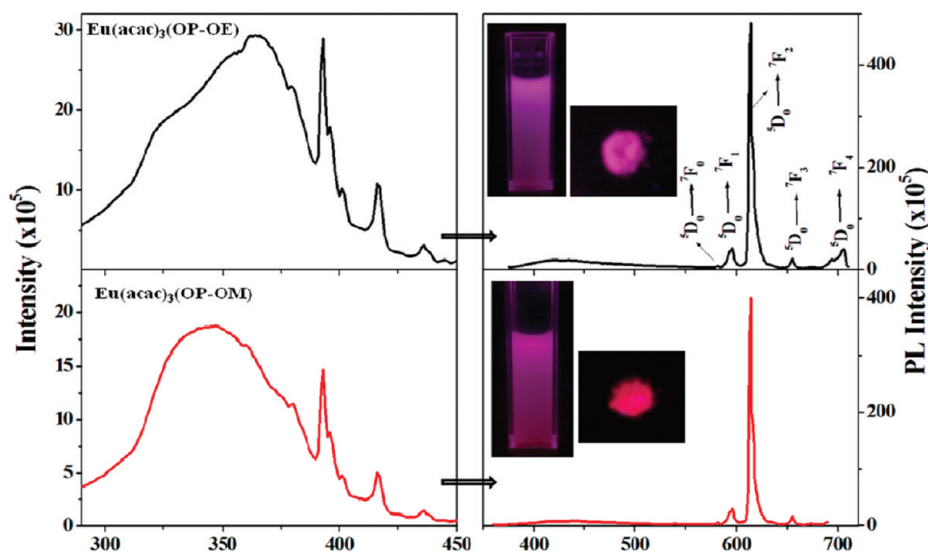


Figure 5. Excitation (left) and emission spectra (right) of oligomer-Eu³⁺ complexes. Emission spectra are recorded using excitation wavelengths of 360 and 340 nm for OP-OE and OP-OM complexes, respectively. The photographs showed their emission both in powder form and dispersed in dimethylsulfoxide.

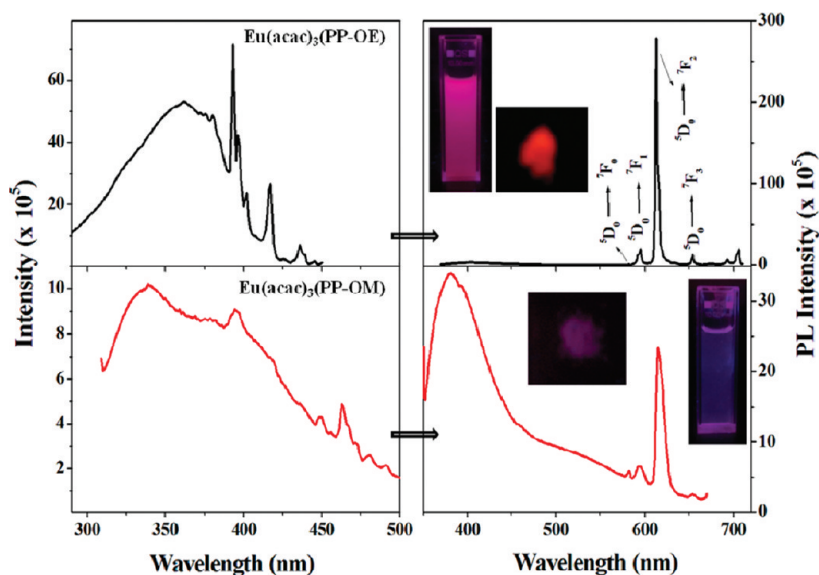


Figure 6. Excitation (left) and emission spectra (right) of polymer-Eu³⁺ complexes. Emission spectra are recorded using excitation wavelengths of 360 and 340 nm for PP-OE and PP-OM complexes, respectively. The photographs showed their emission both in powder form and dispersed in dimethylsulfoxide.

perfect red-color emission ($x = 0.65$ and $y = 0.35$).^{2,27} The oligomer complexes OP-OE ($x = 0.47$ and $y = 0.26$) and OP-OM ($x = 0.53$ and $y = 0.28$) showed coordinates similar to the magenta color. On the other hand, the methoxy polymer complex showed predominantly blue emission ($x = 0.29$ and $y = 0.25$) from the polymer backbone rather than the metal center.

Photoluminescence Lifetime. Luminescent decay lifetime measurements of the complexes were carried out by a pulsed tungsten lamp at room temperature (298 K). The luminescent decay profiles are shown in the Supporting Information (see Figure S16), and lifetime values are given in Table 1. The decay profile curves of Eu³⁺ complexes are fitted with first-order exponential decay. These results indicate that each Eu³⁺ complex

has a single chemical environment around the Eu³⁺ ion. The methoxy polymer showed relatively fast decay compared to other three complexes (see Figure S16). Both oligomers and PP-OE polymer complexes showed lifetime values in the range of 800 μ s.²⁸ The methoxy polymer PP-OM showed the lifetime as 170 μ s, which is almost four times lower compared to other complexes. This low lifetime of the methoxy polymer complex is attributed to the partial excitation energy loss via self-emission rather than transfer to metal center. To find out the role of the temperature on the luminescent lifetimes, the decay data were also recorded at -77 °C. The lifetime values were found to be almost similar to that of those measured at 25 °C. The intrinsic emission quantum yield (ϕ_{Ln}) of the ⁵D₀ excited state (Eu³⁺ ion)

Table 1. Energy Levels, Fluorescent Life Time Rate Constants, and Intrinsic Quantum Yields of the Complexes

complexes	$A_{\text{RAD}} (s^{-1})$	$A_{\text{NR}} (s^{-1})$	$\tau (\mu s)$		$\phi_{\text{Ln}} (\%)$	singlet state (cm^{-1})	triplet state (cm^{-1})
			${}^5\text{D}_0$ at 298 K (τ_{obs})	${}^5\text{D}_0$ calcd. (τ_{rad})			
Eu(acac) ₃ PP-OE	740	510	800 ± 1	1350	59.0	28090	20040
Eu(acac) ₃ PP-OM	290	5400	170 ± 1	3400	5.0	30200	20200
Eu(acac) ₃ OP-OE	420	940	730 ± 3	2380	30.0	30760	21368
Eu(acac) ₃ OP-OM	490	750	805 ± 3	2050	39.0	31740	21140

was calculated from the emission spectra and lifetime measurements of ${}^5\text{D}_0$ emitting level. On the basis of the lifetime data, the radiative decay (A_{RAD}) and nonradiative decay rates were calculated by following the literature procedure (see the Supporting Information for more detail). The calculated values were given in Table 1. Among the Eu^{3+} complexes, $\text{Eu}(\text{acac})_3(\text{PP-OE})$ showed the highest intrinsic quantum yield (ϕ_{Ln}) of 59%. It suggests that PP-OE chains completely transferred energy from conjugated backbone to Eu^{3+} ion for enhanced red emission. The ϕ_{Ln} of the oligomer complexes are just half of the PP-OE complexes, whereas the value is almost 10 times lower for the methoxy polymer PP-OM complex. To further clarify the energy transfer mechanism, singlet and triplet energy levels of polymeric, oligomeric, and monomeric ligands were calculated, and schematic energy transfer diagrams for polymer and oligomers are shown (see Figure S13, Supporting Information). Singlet (${}^1\pi-\pi^*$) and energy levels were obtained from absorption spectra (lower energy absorption edges in Figure 3) of the chromophores. The difference in S_1 energy levels (HOMO) among the polymer and oligomer are very small (only $\sim 1600 \text{ cm}^{-1}$), which suggests that all of the new chromospheres have an almost identical energy state for photoexcitation toward the Eu^{3+} ions. The triplet energy state (${}^3\pi-\pi^*$) was determined from phosphorescence spectra of Gd^{3+} complexes (higher energy emission edges in Figure S12).^{19,29} Calculated values of singlet and triplet state energy levels were given in the Table 1 (see Figure S13 in the Supporting Information for calculation). According to Latva's empirical rule, energy transfer from the ligand to excited state of Eu^{3+} metal ion is more effective when $\Delta E ({}^3\pi\pi^* - {}^5\text{D}_0)$ is equal to $2500-4000 \text{ cm}^{-1}$.³⁰ As shown in Table 1, the energy gap $\Delta E ({}^3\pi\pi^* - {}^5\text{D}_0)$ between the triplet excited state of the ligand and excited state of Eu^{3+} ion is obtained as 2780, 2700, 4000, and 3640 cm^{-1} for PP-OE, PP-OM, OP-OE, and OP-OM, respectively. It is clearly evident that all of the chromophores followed Latva's rule and possessed required energy levels for being as very good sensitizer of the Eu^{3+} metal ion. Despite following Latva's rule, the methoxy substituted rigid polymer did not show complete photoexcitation to the metal centers. Both methoxy (PP-OM) and ethylhexyl (PP-OE) substituted polymers have identical π -conjugated structures in the backbone, and therefore, their difference in the photoexcitation capabilities based on variation in the energy levels is ruled out. The difference in their photosensitizing capabilities may arise from the other features of conjugated polymer such as aromatic π -stacking, and so forth.

Chain Aggregation of Polymer Photosensitizers. In general, π -conjugated polymers possess a high tendency for molecular aggregation via aromatic π -stack interactions.³¹ Thus, studying the aggregation behaviors of the ethylhexyl and methoxy substituted polymers (as sodium salts) could provide more insight into their difference in the photosensitizing capabilities toward Eu^{3+} ions. To trace the aggregation states of the

polymers, the sodium salts of the polymers PP-OE and PP-OM were subjected to DLS and AFM image analysis. DLS histograms of sodium salts of polymers and their AFM images at $1 \times 10^{-6} \text{ M}$ are shown in Figure 7. The DLS plots of the polymer samples showed monomodal distribution with the formation of nanometer size aggregates in water. The formation of the nanoaggregates may be explained based on the unique polyanionic nature of the polymers. The hydrophobicity of the polymers arises from the rigid aromatic *m*-phenylene backbones, and carboxylate anions provide hydrophilicity in the structure.³² As the consequence, the entire polymer gains an amphiphilic nature and self-organizes to produce nanometer size aggregates in water. To further confirm the nature and shape of the aggregates, the AFM images of the samples were recorded for drop cast solutions ($1 \times 10^{-6} \text{ M}$). AFM images of the PP-OM showed the formation of tiny 200 nm size particles, whereas the ethylhexyl substituted polymers (PP-OE) produced mixtures of 500 nm particles with few micrometer size larger aggregates. Both DLS and AFM studies clearly evidence that the size of the aggregates in the ethylhexyl polymer (PP-OE- Na^+) is almost double compared to that of its methoxy substituted polymer counterpart (PP-OM- Na^+). The size-dependent self-organizations of the polymers are schematically shown in Figure 8. The formation of the large size aggregates in PP-OE polymer correlated to the loose packing of the aryl backbone due to the steric hindrance introduced by the ethylhexyl unit. Further, the branched ethylhexyl units are hydrophobic and prefer to occupy the central core of the aggregates rather than project outward in the aqueous medium. On the other hand, the carboxylate anion is hydrophilic and preferentially occupies the periphery of the aggregates. In the case of the methoxy substituted polymer, the hydrophobic volume (or steric hindrance) provided by the anchoring unit is almost negligible, and PP-OM chains are highly rigid and tightly packed to produce tiny nanoaggregates of 200 nm. The roles of the methoxy and ethylhexyl units on the packing of the polymer chains were further evident from the photophysical characteristics of the polymer samples (see Figure 3). The loosely packed ethylhexyl polymer possessed a high possibility for interchain interactions; as a result, both the absorbance and the emission spectra were red-shifted compared to that of the methoxy polymer. Hence, all three independent studies such as DLS, AFM, and emission confirmed the variation in the molecular self-organization among the methoxy and ethylhexyl polymers in water.

Mechanism of Photosensitization Process. On the basis of the above studies, the mechanisms for the variation in the photosensitizing behavior of methoxy and ethylhexyl polymer are proposed in Figure 8. During the complex formation, the $\text{Eu}(\text{acac})_3$ metal center interacts with the sodium carboxylate functionality in water to produce the polymer- $\text{Eu}(\text{acac})_3$ complexes. In the present case, the metal ions could interact with the

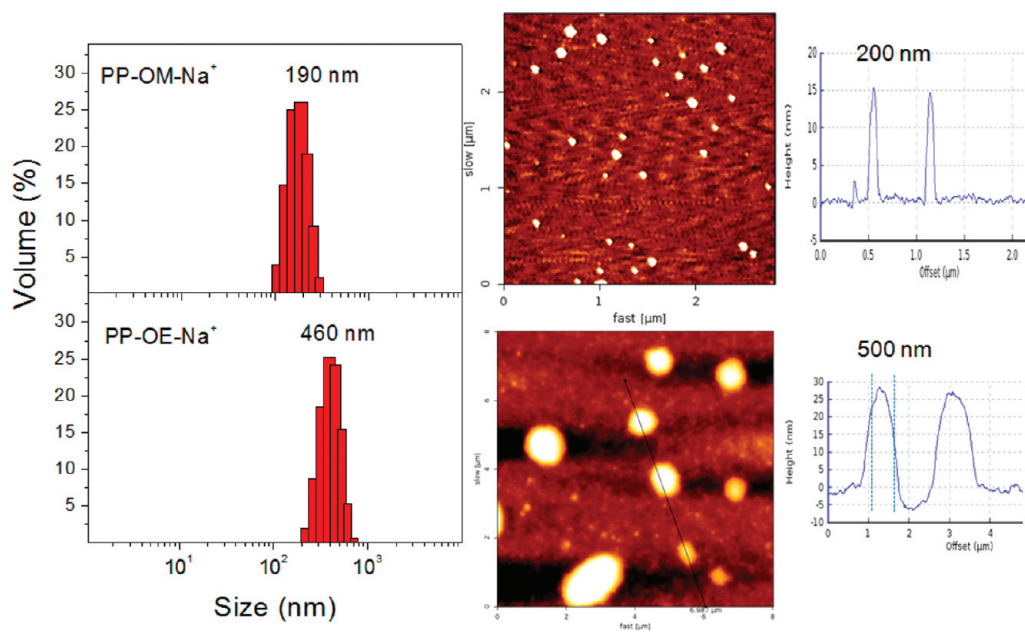


Figure 7. DLS histograms and AFM images of PP-OM-Na⁺ and PP-OE-Na⁺.

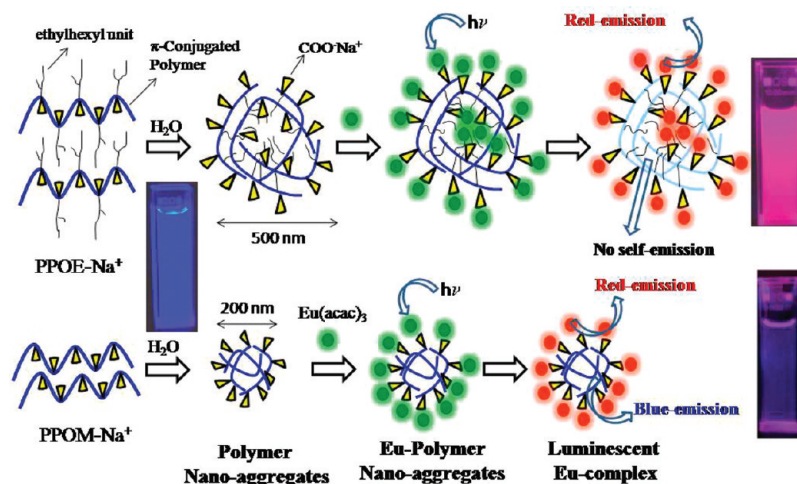


Figure 8. Schematic representation of the mechanism of photosensitizing of PP-OM-Na⁺ and PP-OE-Na⁺.

carboxylic groups both at peripheries as well as the interior of the nanoaggregates. The loosely packed sodium salt of the ethylhexyl polymers provides a larger cavity at the center of the aggregates which facilitate the penetration of the metal ions into both center as well as periphery. In the subsequent photoexcitation, the energy transfer from the polymer backbone to the Eu³⁺ ion occurred at all of the sites of the nanoaggregates both interior as well as in the periphery. As a result, the excitation energy is completely transferred from the polymeric ligand to metal center, and bright red emission was obtained (see Figure 6) with a very high intrinsic quantum yield of 59%. In the case of the methoxy polymer, the rigid tightly packed polymer backbone resists the entry of the Eu³⁺ ion to the core of the nanoaggregates. Hence, the Eu³⁺ ion could only bind to the periphery of the tiny nanoaggregates. During the photoexcitation, the excitation energy transfer from the polymer chain at the exterior to the metal ion results in the red emission. However, the absence of metal ions in the tightly packed interior

portion of the aggregates promotes self-emission of the polymer chains (blue color) rather than sensitizing the Eu³⁺ ions. As a consequence the emission spectrum of the methoxy polymer-Eu³⁺ ion complex showed weak metal center emission with a very low intrinsic quantum yield (5%). The variation in the photosensitizing abilities among the polymer chromophores (methoxy versus ethylhexyl substituted chains) are directly correlated to the nanoaggregates of the polymers in the solution. Loosely packed larger nanoaggregates are better photosensitizers compared to that of the tightly packed tiny particles. Both oligomer complexes were found to be almost identical with a relatively low intrinsic quantum yield of 31%. The present studies prove that the macromolecular chromophores are superior photosensitizers for Eu³⁺ ions compared to their oligomers. It is very important to design an appropriate polymer backbone with suitable anchoring groups for efficient and successful emission based on conjugated polymer-lanthanide hybrid materials.

CONCLUSIONS

In conclusion, we have designed and synthesized new classes of π -conjugated oligomers and polymers based on poly(phenylene)s having carboxylic acid functional groups and utilized them successfully as efficient photosensitizers for Eu^{3+} ions. The importance of the present investigation is summarized as follows: (i) new oligo-phenylenes and poly(phenylene)s were synthesized based on phenylpropionic acid monomers via a palladium mediated Suzuki polycondensation route, (ii) the polymer backbone was anchored with methoxy and ethylhexyl units to study their effect on the molecular weight formation and photosensitization, (iii) the ethylhexyl units enhance the molecular weight of the polymers in the Suzuki polycondensation reaction, (iv) the photophysical studies revealed that the ethylhexyl polymer possessed strong interchain interactions and the spectra were red-shifted compared to other derivatives, (v) both oligomer and polymer showed high selectivity toward the photosensitization toward Eu^{3+} ions compared to other lanthanides, (iv) the oligomer complexes showed magenta color emission due to the combination of weak self-emission from the chromophores and strong red emission from the metal center, (vii) the photosensitizing capabilities of the polymers were found highly selective toward their structure: the ethylhexyl substituted polymer showed complete energy transfer from chromophores and produce sharp red emission, whereas its methoxy counterpart was found not suitable, (viii) photoluminescent lifetime measurements and the energy level calculation based on Latva's rule revealed that the reason for the difference in the photosensitization of polymers reside on their molecular self-organization, (ix) DLS and AFM studies confirmed the existence of nanoaggregates for the polymer structure, (x) the ethylhexyl polymer produced loosely packed aggregates for efficient binding of the metal ions, (xi) the methoxy polymer produced tightly packed nanoaggregates and showed largely self-emission, and (xii) the size and shape of the polymer chain aggregates in water are found to play a crucial role on the photosensitization of polymeric chromophores. The carboxylic functionalized π -conjugated poly(phenylene) design provides a new opportunity for tuning the color of the lanthanide complexes which may find potential applications in opto-electronics. In a nut shell, in the present investigation, for the first time, new carboxylic acid functionalized oligo and poly(phenylene)s were synthesized to trace the superiority of the photosensitizing properties of the macromolecular chain over the small derivatives in lanthanide complexes.

ASSOCIATED CONTENT

S Supporting Information. Structural characterization data of monomers by ^1H NMR, ^{13}C NMR, IR, and MALDI-TOF-TOF spectra, 2D-NMR spectra of IR, TGA thermograms, energy level diagram, and phosphorescence spectra of oligomers and polymers. This material is available free of charge via the Internet at <http://pubs.acs.org>.

AUTHOR INFORMATION

Corresponding Author

*E-mail: jayakannan@iiserpune.ac.in.

ACKNOWLEDGMENT

We thank Department of Science of Technology, New Delhi, India under Scheme: NSTI Programme-SR/NM/NS-42/2009

and SR/S1/OC-54/2009 for financial support. A.B. thanks CSIR-New Delhi, India for a senior research fellowship.

REFERENCES

- (1) (a) Pei, J.; Liu, X. L.; Yu, W. L.; Lai, Y. H.; Niu, Y. H.; Cao, Y. *Macromolecules* **2002**, *35*, 7274–7280. (b) Robinson, M. R.; Ostrowski, J. C.; Bazan, G. C.; McGehee, M. D. *Adv. Mater.* **2003**, *15*, 1547–1551.
- (2) Giovanella, U.; Pasini, M.; Freund, C.; Botta, C.; Porzio, W.; Destri, S. *J. Phys. Chem. C* **2009**, *113*, 2290–2295.
- (3) (a) Forrest, S. R. *Nature* **2004**, *428*, 911–918. (b) Gustafsson, G.; Cao, Y.; Treasy, G. M.; Klavetter, F.; Colaneri, N.; Heeger, A. J. *Nature* **1992**, *357*, 477–479.
- (4) Bettencourt-Dias, A. D. *Dalton Trans.* **2007**, 2229–2241.
- (5) Kido, J.; Okamoto, Y. *Chem. Rev.* **2002**, *102*, 2357–2368.
- (6) Eliseeva, S. V.; Bunzli, J. C. G. *Chem. Soc. Rev.* **2010**, *39*, 189–227.
- (7) Binnemans, K. *Chem. Rev.* **2009**, *102*, 4283–4374.
- (8) McGehee, M. D.; Bergstedt, T.; Zhang, C.; Saab, A. P.; O'Regan, M. B.; Bazan, G. C.; Srdanov, V. I.; Heeger, A. J. *Adv. Mater.* **1999**, *11*, 1349–1354.
- (9) Kang, T. S.; Harrison, B. S.; Bouguettaya, M.; Foley, T. J.; Boncella, J. M.; Schanze, K. S.; Reynolds, J. R. *Adv. Funct. Mater.* **2003**, *13*, 205–210.
- (10) Harrison, B. S.; Foley, T. J.; Bouguettaya, M.; Boncella, J. M.; Schanze, K. S.; Reynolds, J. R.; Shim, J.; Holloway, P. H.; Padmanaban, G.; Ramakrishnan, S. *Appl. Phys. Lett.* **2001**, *79*, 3770–3773.
- (11) (a) Chen, X. Y.; Yang, X.; Holliday, B. J. *J. Am. Chem. Soc.* **2008**, *130*, 1546–1547. (b) Shunmugam, R.; Tew, G. N. *J. Am. Chem. Soc.* **2002**, *127*, 13567–13572.
- (12) (a) Song, Y.; Tan, Y. P.; Teo, E. Y. H.; Zhu, C.; Chan, D. S. H.; Ling, Q. D.; Neoh, K. G.; Kang, E. T. *J. Appl. Phys.* **2006**, *100*, 0845081–0845086. (b) Shunmugam, R.; Tew, G. N. *Polym. Adv. Technol.* **2008**, *19*, 596–601.
- (13) (a) Zhang, Z. G.; Yuan, J. B.; Tang, H. J.; Tang, H.; Wang, L. N.; Zhang, K. L. *J. Polym. Sci., Part A: Polym. Chem.* **2009**, *47*, 210–221. (b) Ling, Q. D.; Wang, W.; Song, Y.; Zhu, C. X.; Chan, D. S. H.; Kang, E. T.; Neoh, K. G. *J. Phys. Chem. B* **2006**, *110*, 23995–24001. (c) Xu, C. J.; Li, B. G. *Macromol. Chem. Phys.* **2010**, *211*, 1733–1740.
- (14) (a) Kang, T. S.; Harrison, B. S.; Foley, T. J.; Knefely, A. S.; Boncella, J. M.; Schanze, K. S.; Reynolds, J. R. *Adv. Mater.* **2003**, *15*, 1093–1097. (b) Yong, Z.; Lei, W.; Chun, L.; Jin, Z. W.; Hong, S. H.; Yong, C. *Chin. Phys. Lett.* **2007**, *24*, 1376–1379.
- (15) Velasco, D. S.; de Moura, A. P.; Medina, A. N.; Baesso, M. L.; Rubira, A. F.; Cremona, M.; Bento, A. C. *J. Phys. Chem. B* **2010**, *114*, 5657–5660.
- (16) Ling, Q. D.; Kang, E. T.; Neoh, K. G. *Macromolecules* **2003**, *36*, 6995–7003.
- (17) (a) Wen, G. A.; Zhu, X. R.; Wang, L. H.; Feng, J. C.; Zhu, R.; Wei, W.; Peng, B.; Pei, Q. B.; Huang, W. J. *Polym. Sci., Part A: Polym. Chem.* **2007**, *45*, 388–394. (b) Wong, K. S.; Sun, T.; Liu, X. L.; Pei, J.; Huang, W. *Thin Solid Films* **2002**, *417*, 85–89. (c) Cheng, Y.; Zou, X.; Zhu, D.; Zhu, T.; Liu, Y.; Zhang, S.; Huang, H. *J. Polym. Sci., Part A: Polym. Chem.* **2007**, *45*, 650–660.
- (18) (a) Yong, Z.; Hong, S. H.; Yong, C. *Chin. J. Chem.* **2006**, *24*, 1631–1638. (b) Qian, W.; Chaofan, Z.; Rongfang, G.; Aihong, H.; Hualiang, H. *J. Rare Earths* **2007**, *25*, 562–507. (c) Ambili Raj, D. B.; Biju, F.; Reddy, M. L. P.; Butorac, R. R.; Lynch, V. M.; Cowley, A. H. *Inorg. Chem.* **2010**, *49*, 9055–9063. (d) Biju, S.; Reddy, M. L. P.; Cowley, A. H.; Vasudevan, K. V. *J. Mater. Chem.* **2009**, *19*, 5179–5187.
- (19) (a) Oxley, D. S.; Walters, R. W.; Copenhafer, J. E.; Meyer, T. Y.; Petoud, S.; Edenborn, H. M. *Inorg. Chem.* **2009**, *48*, 6332–6334. (b) Liu, Y.; Wang, Y.; Guo, H.; Zhu, M.; Li, C.; Peng, J.; Zhu, W.; Cao, Y. *J. Phys. Chem. C* **2011**, *115*, 4209–4216.
- (20) (a) Stanley, J. M.; Zhu, X.; Yang, X.; Holliday, B. J. *Inorg. Chem.* **2010**, *49*, 2035–2037. (b) Chandrasekhar, N.; Chandrasekar, R. *J. Org. Chem.* **2010**, *75*, 4852–4855. (c) Latva, M.; Takalo, H.; Simberg, K.; Kankare, J. *J. Chem. Soc., Perkin Trans.* **1995**, *2*, 995–999.

(21) (a) Wolbers, M. P.O.; Veggel, F. C. J. M. V.; Hofstraat, J. W.; Geurts, F. A. J.; Reinhoudt, D. N. *J. Chem. Soc., Perkin Trans.* **1997**, *2*, 2275–2282. (b) Destri, S.; Porzio, W.; Meinardi, F.; Tubino, R.; Salerno, G. *Macromolecules* **2003**, *36*, 273–275.

(22) (a) Sato, S.; Wada, M. *Bull. Chem. Soc. Jpn.* **2007**, *22*, 1955–1962. (b) Bhaumik, M. L.; Sayed, M. A. E. *J. Chem. Phys.* **1965**, *42*, 787–788. (c) Crosby, G. A.; Whan, R. E.; Alire, R. M. *J. Chem. Phys.* **1961**, *34*, 743–748.

(23) Balamurugan, A.; Reddy, M. L. P.; Jayakannan, M. *J. Phys. Chem. B* **2009**, *113*, 14128–14138.

(24) (a) Anish, C.; Amrutha, S.; Jayakannan, M. *J. Polym. Sci., Polym. Chem.* **2008**, *46*, 3241–3256. (b) Liao, L.; Pang, Y.; Ding, L.; Karasz, F. E. *Macromolecules* **2001**, *34*, 7300–7305. (c) Liao, L.; Pang, Y. *Synth. Met.* **2004**, *144*, 271–277. (d) Drury, A.; Maier, S.; Davey, A. P.; Dalton, A. B.; Coleman, J. N.; Byrne, H. J.; Blau, W. J. *Synth. Met.* **2001**, *119*, 151–152. (e) Liang, H.; Yan, J.; Lu, J. *Synth. Met.* **2004**, *142*, 143–145. (f) Mahler, A. K.; Schlick, H.; Saf, R.; Stelzer, F.; Meghdadi, F.; Pogantsch, A.; Leising, G.; Moller, K. C.; Besanhard, J. O. *Macromol. Chem. Phys.* **2004**, *205*, 1840–1850.

(25) Shyni, R.; Reddy, M. L. P.; Cowley, A. H.; Findlater, M. *Eur. J. Inorg. Chem.* **2008**, *2008*, 4387–4394.

(26) (a) Shyni, R.; Biju, S.; Reddy, M. L. P.; Cowley, A. H.; Findlater, M. *Inorg. Chem.* **2007**, *46*, 11025–11030. (b) Pavithran, R.; Saleesh Kumar, N. S.; Biju, S.; Reddy, M. L. P.; Junior, S. A.; Freire, R. O. *Inorg. Chem.* **2006**, *45*, 2184–2192. (c) Biju, S.; Ambili Raj, D. B.; Reddy, M. L. P.; Kariuki, B. M. *Inorg. Chem.* **2006**, *45*, 10651–10660.

(27) Lidia Armelao, L.; Bottaro, G.; Quici, S.; Cavazzini, M.; Concetta Raffo, M.; Barigelletti, F.; Accorsi, G. *Chem. Commun.* **2007**, 2911–2193.

(28) Werts, M. H. V.; Jukes, R. T. F.; Verhoeven, J. W. *Phys. Chem. Chem. Phys.* **2002**, *4*, 1542–1548.

(29) (a) Shi, M.; Li, F.; Yi, T.; Zhang, D.; Hu, H.; Huang, C. *Inorg. Chem.* **2005**, *44*, 8929–8936. (b) Xin, H.; Shi, M.; Gao, X. C.; Huang, Y. Y.; Gong, Z. L.; Nie, D. B.; Cao, H.; Bian, Z. Q.; Li, F. Y.; Huang, C. H. *J. Phys. Chem. B* **2004**, *108*, 10796–10800.

(30) Latva, M.; Takalo, H.; Mukkala, V. M.; Matachescu, C.; Rodriguez-Ubis, J. C.; Kanakare, J. *J. Lumin.* **1997**, *75*, 149–169.

(31) (a) Amrutha, S. R.; Jayakannan, M. *J. Phys. Chem. B* **2006**, *110*, 4083–4091. (b) Amrutha, S. R.; Jayakannan, M. *J. Phys. Chem. B* **2008**, *112*, 1119–1129. (c) Amrutha, S. R.; Jayakannan, M. *Macromolecules* **2007**, *40*, 2380–2391. (d) Resmi, R.; Amrutha, S. R.; Jayakannan, M. *J. Polym. Sci., Polym. Chem.* **2009**, *47*, 2631–2341.

(32) (a) Balamurugan, A.; Reddy, M. L. P.; Jayakannan, M. *J. Polym. Sci., Polym. Chem.* **2009**, *47*, 5144–5157. (b) Jiang, H.; Taranekar, P.; Reynolds, J. R.; Schanze, K. S. *Angew. Chem., Int. Ed.* **2009**, *48*, 4300–4316.